Journal of Materials Chemistry

Cite this: J. Mater. Chem., 2011, 21, 13772

www.rsc.org/materials

COMMUNICATION

Dependence of structures and properties of carbon nanotube fibers on heating treatment†

Zhibin Yang,[abc] Xuemei Sun,[abc] Xuli Chen,[abc] Zhenzhong Yong,[d] Gen Xu,[d] Ruixuan He,[abc] Zhenghua An,[c] Qingwen Li*[d] and Huisheng Peng*[a]

Received 26th May 2011, Accepted 8th July 2011
DOI: 10.1039/c1jm12346g

The dependence of structures and mechanical and electrical properties of carbon nanotube fibers on heating treatments have been first investigated in both argon and air. The relationships between structures and properties have been also explored. These discoveries may be used to design and improve carbon nanotube fibers.

In order to improve their practical applications, carbon nanotubes (CNTs) have been widely assembled into macroscopic fibers.[1,2] As CNTs are highly aligned with each other, the resulting fibers maintain the remarkable physical properties of individual CNTs. For instance, CNT fibers are ultralight and flexible, and they exhibit excellent mechanical and electrical properties.[3–10] The significant mechanical properties suggest them as a high-performance structural materials. CNT fibers can also achieve high electrical conductivities on level of 10^3 S cm^{-1},[9] which enables promising applications as a new family of electrodes in a broad spectrum of optoelectronic devices.[10–13]

A lot of effort has been previously paid to preparation of CNT fibers. Three main fabrication processes, *i.e.*, wet spinning,[14] dry spinning,[1,15–19] and direct spinning from a chemical vapor deposition reactor,[20,21] have been developed to spin CNT fibers. Recently, increasing interest has been attracted to further tune their structures and improve their mechanical and electrical properties to meet more applications. It is found that the longer the CNTs, the higher the mechanical strength and electrical conductivity of the resulting fibers.[22] In addition, a wide variety of inorganic and organic moieties have been incorporated to form composite fibers to improve mechanical and electrical properties.[4,23] However, to the best of our knowledge, few studies have been made to investigate the temperature dependence of CNT fibers. On the other hand, this is a critical issue as they may be used in various fields with a wide temperature range. In addition, it is also easy and effective to perform heating treatment on CNT fibers aiming at controlled structures and properties required by many practical applications.

Herein, we have carefully studied heating effects on structures and mechanical and electrical properties of CNT fibers. Two different heating models, one in argon and another in air, are investigated and compared. It is found that values of D-band to G-band (I_D/I_G) in CNT fibers almost continuously decreases with increasing heating temperatures from 25 to 900 °C in argon, while the I_D/I_G values show a minimum value at 300 °C in heating temperature range of 25 to 400 °C in air. Interestingly, specific strengths of CNT fibers exhibit the highest value at 300 °C in both argon and air, and their electrical conductivities continuously decrease with increasing heating temperatures. Experiments and discussions are provided to explain the above phenomena.

Experimental section

Preparation and heating treatment of CNT fibers

CNTs were synthesized by a typical chemical vapor deposition in a quartz tube furnace using Fe/Al_2O_3 on silicon wafer as the catalyst.[24–26] The synthetic details of CNTs as well as their spinning into fibers have been reported elsewhere.[27] The rotation speeds of the microprobe ranged from 2000 to 6000 rad min^{-1} during the spinning process. Heating treatments in air and argon were performed by putting CNT fibers on a hot plate and into a quartz tube furnace for 30 min, respectively.

Characterizations

Raman measurements were made at Renishaw in Via Reflex with excitation wavelength of 514.5 nm and laser power of 20 mW at room temperature. CNT structure was characterized by transmission electron microscopy (TEM, JEOL JEM-2100F operated at 200 kV), and fiber structure was analyzed by scanning electron microscopy (SEM, Shimadz SUPERSCAN SSX-550 operated at 15 kV). Mechanical tests were performed on a Hengyi Table-Top Universal Testing Instrument. The fiber samples were mounted on paper tabs with a gauge length of 5 mm, and their diameters were determined by SEM. Electrical characterizations were made through four-probe method (KEITHLEY 2182A nanocoltmeter with 6221A DC and AC current source).

[a]*Key Laboratory of Molecular Engineering of Polymers of Ministry of Education, Shanghai, 200438, China*
[b]*Department of Macromolecular Science, Shanghai, 200438, China*
[c]*Laboratory of Advanced Materials, Fudan University, Shanghai, 200438, China. E-mail: penghs@fudan.edu.cn*
[d]*Suzhou Institute of Nano-Tech and Nano-Bionics, Jiangsu, 215123, China. E-mail: qwli2007@sinano.ac.cn.*
† Electronic supplementary information (ESI) available. See DOI: 10.1039/c1jm12346g

Results and discussion

CNT arrays were first synthesized by using Fe/Al_2O_3 as catalyst through a chemical vapor deposition process, and CNT fibers had been directly spun from these arrays. Fig. 1a shows a scanning electron microscopy (SEM) image of a CNT fiber. The fiber was uniform in diameter along the axial direction. In addition, it was flexible and did not break after being bent many times. Fig. 1b shows a high-resolution transmission electron microscopy (TEM) image of a CNT in the array which was spun into fiber. It indicates a multi-walled structure with diameter of ~12 nm.

Firstly, we have studied the heating effect on structures and mechanical and electrical properties of CNT fibers at a temperature range from 25 to 900 °C in argon. The structure varieties were carefully traced by Raman spectroscopy. Fig. 2a shows normalized Raman spectra (intensities of G-band are normalized to be the same) of as-synthesized and treated CNT fibers with different temperatures of 100, 200, 300, 400, 500, 600, 700, 800, and 900 °C. D-band and G-band are located at ~1350 cm^{-1} and ~1580 cm^{-1}, respectively. I_D/I_G values have been further compared in Fig. 2b. I_D/I_G continuously decreases with increasing temperatures from 25 to 900 °C. It is well known that D-band and G-band in pure CNTs correspond to their defects or disorder of graphene sheets and C–C stretching (E_{2g}) model of graphite, respectively, and the intensity ratio of D-band to G-band reflects their crystallinity degree. During synthesis of CNT arrays for preparation of fibers, carbon-based impurities such as amorphous carbon are also produced on the outer surfaces of CNTs. Therefore, both CNTs and impurities contribute to the peak intensities of D-band and G-band in Raman spectra. According to the TEM observations in Fig. S1 (ESI†), impurities such as amorphous carbon were not removed during the heating treatment in argon, while some defects in CNTs were further healed to show better crystallinity with decreasing I_D/I_G values. Therefore, a continuous decrease of I_D/I_G (intensity ratio of D-band to G-band) values with increasing treatment temperatures was detected. It should be noted that the healing reactions of defects may occur even at low temperature of 100 °C as the I_D/I_G value obviously decreases after heating treating treatment at this point. Alignment of CNTs and length of CNT fibers were characterized by SEM and optical microscopy, respectively, and Fig. S2 and S3 show that both of them remain the same during heating treatments at different temperatures. However, Fig. S4 shows that diameters of CNT fiber obviously increase with increasing treatment temperatures.

Dependence of mechanical and electrical properties on temperature has been studied by comparing specific strengths and electrical conductivities of CNT fibers under heating treatments at different temperatures. Interestingly, different from the almost linear decrease of I_D/I_G values, specific strengths do not continuously increase or decrease with increasing treatment temperatures. Fig. 2c shows that average specific strengths of CNT fibers treated in air increase from 1.77 to 2.78 GPa g^{-1} cm^3 (by ~57%) from 25 to 300 °C and then decrease to 1.26 GPa g^{-1} cm^3 (by ~55%) with a further increase of treatment temperature to 900 °C. As widely investigated, individual CNTs are the strongest material ever discovered by human kind, and CNT fibers are broken mainly due to the slide among neighboring CNTs which are attached with each other through van der Waals forces. Therefore, their specific strengths reflect interactions among neighboring CNTs. In other words, stronger interactions produce higher strengths. Herein, two opposite parameters, *i.e.*, integrity of CNTs and change of CNT density, may contribute to interactions among neighboring CNTs in fibers. More CNT defects are healed to improve their interactions while decreasing CNT densities (or increasing diameters shown in Fig. S4, ESI†) reduce their interactions with increasing treatment temperatures. The first contribution exceeds the second one below 300 °C, and the second exceeds the first at higher temperatures, so a peak value of specific strength is observed in CNT fiber. Fig. S5 (ESI†) further supports the above conclusion by comparing dispersions of CNT fibers before and after heating treatments with increasing temperatures. Under the same experimental conditions, CNTs treated at 300 °C are more difficult to disperse in ethanol than those without treatment or treated at higher temperature of 900 °C. Electrical resistances of CNT fibers are composed of two main parts, *i.e.*, resistances of individual CNTs and contact resistances among CNTs. Therefore, integrity and distance of CNTs also oppositely change electrical resistances of CNT fibers. CNTs with less defects decrease individual resistances, while their larger distances increase contacting resistances. Fig. 2d indicates that electrical conductivities continuously decrease with increasing treatment temperatures. In other words, the above change is dominated by the first factor.

In addition, we have also studied heating effects on CNT fibers at a temperature range of 25 to 400 °C in air to mimic their practical applications. The structure varieties were traced by Raman spectroscopy, and two main peaks at about 1350 (D-band) and 1580 (G-band) cm^{-1} are compared in Fig. 3a. It can be found that intensities of D-band decrease from 25 to 300 °C and then increase with increasing temperatures to 400 °C when intensities of G-band are normalized to be the same. Fig. 3b further summarizes I_D/I_G values on the basis of data from Fig. 3a. Different from the case in argon, I_D/I_G values gradually decrease from 0.72 to 0.57 when the treatment temperatures increase from 25 to 300 °C, while rapidly increase to 0.85 at a higher treatment temperature of 400 °C.

Similar to heating treatments in argon, CNT defects are healed in air to improve their crystallinity with decreasing I_D/I_G values. However, deterioration of CNT defects will also occur and accelerate to increase I_D/I_G values with increasing temperatures due to existence of oxygen. This process under heating has not been found for them in argon. The TEM observations in Fig. S6 confirm deterioration of CNT defects. The TGA graph in Fig. S7 shows that impurities such as amorphous carbon on CNTs are maintained during the heating process, which had been observed at similar heating temperatures by other groups.[28–30] Therefore, these impurities do not contribute to the varieties of I_D/I_G values. It may be concluded that the changes of I_D/I_G values are dominated by the first factor from room temperature to 300 °C and by the second factor above 300 °C based on Fig. 3b.

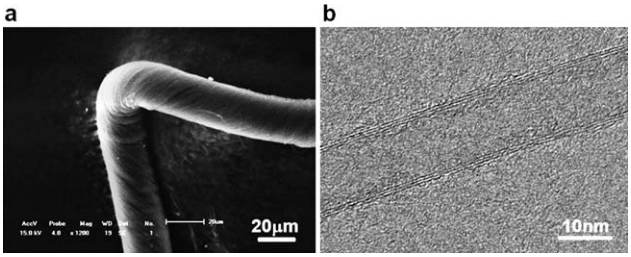

Fig. 1 a. SEM image of a CNT fiber. b. High-resolution TEM image of a CNT.

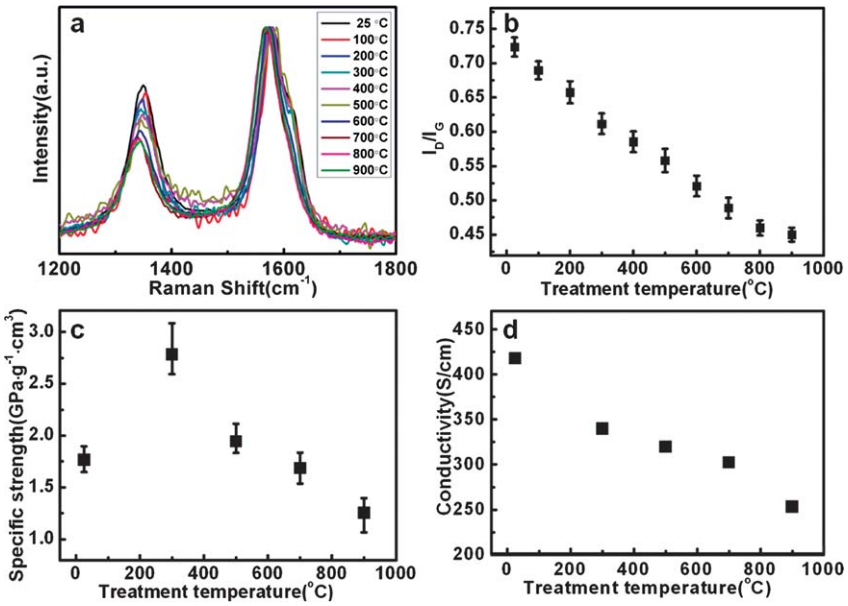

Fig. 2 Structure characterizations of CNT fibers after being heated from 25 to 900 °C in argon. a. Raman spectra. b. Intensity ratios of D-band to G-band. c. Dependence of specific strength on temperature. d. Dependence of electrical conductivity (along the axial direction) on temperature.

TEM observations also support the above conclusion by comparing CNTs before and after heating treatments. Further efforts are required to provide more details.

Similar to CNT fibers treated in argon, alignment of CNTs and length of CNT fibers are maintained after heating treatments with different temperatures, while diameters of CNT fibers obviously increase in air (Fig. S8–S10). Fig. S11 also indicates that CNT fibers can be best dispersed in ethanol under heating treatment of ~300 °C. In addition, average specific strengths of CNT fibers treated in air increase from 1.77 to 2.32 GPa g^{-1} cm^3 (by ~31%) when treatment temperatures rise from 25 to 300 °C and then decrease to 1.82 GPa g^{-1} cm^3 (by ~22%) with a further increase of treatment temperature to 400 °C (Fig. 3c). Of course, two opposite parameters, *i.e.*, integrity of CNTs and change of CNT density, also contribute to interactions among neighboring CNTs in fibers. Besides them, a new third factor of deterioration of CNT defects decreases interactions among CNTs. Therefore, the increased degree of average specific strength from 0 to 300 °C and decreased degree of average specific strength from 300

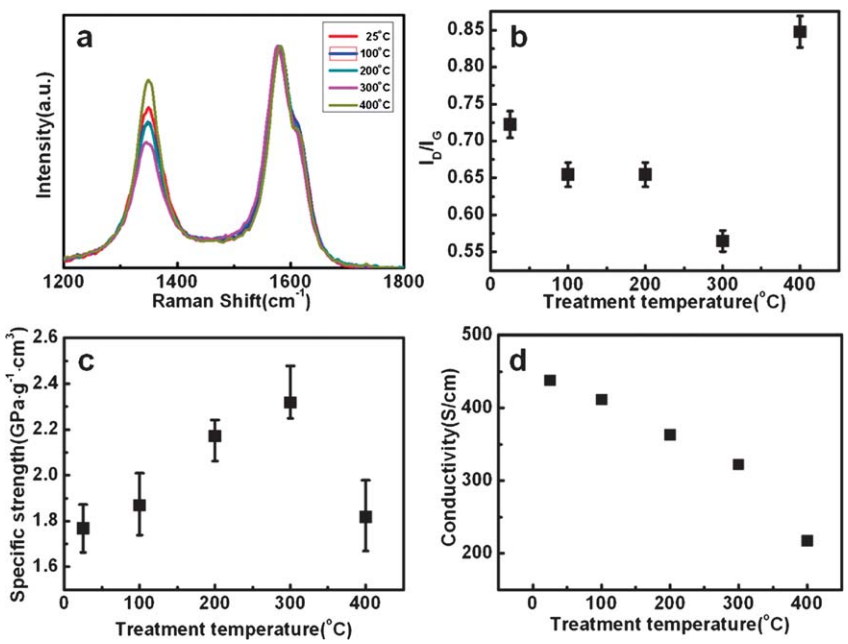

Fig. 3 Structure and property characterizations of CNT fibers after heating treatments in air. a. Raman spectra (peak intensities of G-band are normalized to be the same here). b. Intensity ratios of D-band to G-band. c. Dependence of specific strength on temperature. d. Dependence of electrical conductivity (along the axial direction) on temperature.

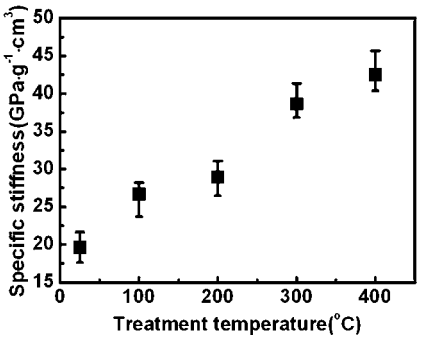

Fig. 4 Fiber's dependence of specific stiffness on temperature in air.

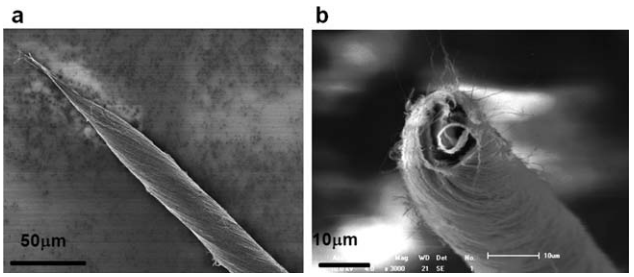

Fig. 5 SEM images of (a) as-synthesized CNT fiber and (b) the treated CNT fiber heated at 300 °C in air.

to 400 °C are lower compared to the heating treatment in argon. However, electrical conductivities continuously decrease with increasing treatment temperatures similar to heating treatments in argon (Fig. 3d).

It is also important to investigate specific toughness of CNT fiber under heating treatments in air. Fig. 4 shows that their specific toughness continuously increases from an average value of 19.64 to 42.48 GPa g^{-1} cm^3 with increasing treatment temperatures from 25 to 400 °C. This phenomenon may be explained by the fact that some defective CNTs were deteriorated to produce more defects in fibers at higher temperatures, and CNT fibers more easily broke from their defects. The enhanced stiffness with increasing treatment temperatures had been also confirmed by SEM observations. We had compared the broken parts of as-synthesized and treated CNT fibers at different temperatures. Fig. 5a exhibits a typical broken end of as-synthesized CNT fiber after a stress-strain test, and the end has been lengthened before breaking. The broken parts became shorter and shorter with increasing treatment temperatures. Fig. 5b shows a broken end of a CNT fiber which was previously heated at 300 °C prior to a mechanical measurement, which indicates a much tougher behavior compared to the as-synthesized CNTs.

Conclusions

In summary, this work reports a careful study of structure and property dependences of CNT fibers on heating treatments with different temperatures in both argon and air. In addition, the relationships between structure and properties in CNT fibers have been also explored. The above discoveries may be used to guide the design and improvement of CNT fibers.

Acknowledgements

This work was supported by Natural National Science Foundation of China (20904006, 91027025), Ministry of Science and Technology (2011CB932503, 2011DFA51330), Science and Technology Commission of Shanghai Municipality (1052nm01600, 09PJ1401100), and Program for New Century Excellent Talents in University (NCET-09-0318), Li Foundation Heritage Prize, and Scientific Research Foundation for the Returned Overseas Chinese Scholars.

Notes and references

1 M. Zhang, K. R. Atkinson and R. H. Baughman, *Science*, 2004, **306**, 1358.
2 K. Jiang, Q. Li and S. Fan, *Nature*, 2002, **419**, 801.
3 H. Peng, M. Jain, Q. Li, D. E. Peterson, Y. Zhu and Q. Jia, *J. Am. Chem. Soc.*, 2008, **130**, 1130.
4 H. Peng, X. Sun, F. Cai, X. Chen, Y. Zhu, G. Liao, D. Chen, Q. Li, Y. Lu, Y. Zhu and Q. Jia, *Nat. Nanotechnol.*, 2009, **4**, 738.
5 M. Sammalkorpi, A. Krasheninnikov, A. Kuronen, K. Nordlund and K. Kaski, *Phys. Rev. B: Condens. Matter Mater. Phys.*, 2004, **70**, 245.
6 S. L. Mielke, D. Troya, S. L. Zhang, J. L. Li, S. P. Xiao, R. Car, R. S. Ruoff, G. C. Schatz and T. Belytschko, *Chem. Phys. Lett.*, 2004, **390**, 413.
7 X. F. Zhang, Q. W. Li, T. G. Holesinger, P. N. Arendt and Y. T. Zhu, *Adv. Mater.*, 2007, **19**, 4198.
8 M. Motta, Y. L. Li, I. Kinloch and A. Windle, *Nano Lett.*, 2005, **5**, 1529.
9 Q. Li, Y. Li, X. Zhang, S. B. Chikkannanavar, Y. Zhao, A. M. Dangelewicz, L. Zheng, S. K. Doorn, Q. Jia, D. E. Peterson, P. N. Arendt and Y. Zhu, *Adv. Mater.*, 2007, **19**, 3358.
10 T. Chen, S. Wang, Z. Yang, Q. Feng, X. Sun, L. Li, Z. Wang and H. Peng, *Angew. Chem., Int. Ed.*, 2011, **50**, 1815.
11 A. B. Dalton, S. Collins, E. Muñoz, J. M. Razal, V. H. Ebron, J. P. Ferraris, J. N. Coleman, B. G. Kim and R. H. Baughman, *Nature*, 2003, **423**, 703.
12 L. Viry, A. Derré, P. Garrigue, N. Sojic, P. Poulin and A. Kuhn, *Anal. Bioanal. Chem.*, 2007, **389**, 499.
13 Z. Zhu, W. Song, K. Burugapalli, F. Moussy, Y. Li and X. Zhong, *Nanotechnology*, 2010, **21**, 165501.
14 L. M. Ericson, H. Fan, H. Peng, V. A. Davis, W. Zhou and J. Sulpizio, *Science*, 2004, **305**, 1447.
15 S. Zhang, Q. Li, Y. Tu, Y. Li, J. Y. Coulter, L. Zheng, Y. Zhao, Q. Jia, D. E. Peterson and Y. Zhu, *Small*, 2007, **3**, 244.
16 E. Y. Jang, T. J. Kang, H. Im, S. J. Baek, S. Kim, D. H. Jeong, Y. W. Park and Y. H. Kim, *Adv. Mater.*, 2009, **21**, 1.
17 J. J. Vilatela and A. H. Windle, *Adv. Mater.*, 2010, **22**, 4959.
18 N. Behabtu, M. J. Green and M. Pasquali, *Nano Today*, 2008, **3**, 24.
19 T. Chou, L. Gao, E. T. Thostenson, Z. Zhang and J. H. Byun, *Compos. Sci. Technol.*, 2010, **70**, 1.
20 X. H. Zhong, Y. L. Li, Y. K. Liu, X. H. Qiao, Y. Feng, J. Liang, J. Jin, L. Zhu, F. Hou and J. Y. Li, *Adv. Mater.*, 2010, **22**, 692.
21 K. Koziol, J. Vilatela, A. Moisala, M. Motta, P. Cunniff, M. Sennett and A. Windle, *Science*, 2007, **318**, 1892.
22 X. Zhang, Q. Li, Y. Tu, Y. Li, J. Y. Coulter, L. Zheng, Y. Zhao and Y. Zhu, *Small*, 2007, **3**, 244.
23 H. Peng, J. Menka, D. E. Peterson, Y. Zhu and Q. Jia, *Small*, 2008, **4**, 1964.
24 H. Peng and X. Sun, *Chem. Commun.*, 2009, 1058.
25 H. Peng, *J. Am. Chem. Soc.*, 2008, **130**, 42.
26 H. Peng and X. Sun, *Chem. Phys. Lett.*, 2009, **471**, 103.
27 J. Zhao, X. Zhang, J. Di, G. Xu, X. Yang, X. Liu, Z. Yong, M. Chen and Q. Li, *Small*, 2010, **6**, 2612.
28 R. Brukh and S. Mitra, *J. Mater. Chem.*, 2007, **17**, 619.
29 N. Dementev, S. Osswald, Y. Gogotsi and E. Borguet, *J. Mater. Chem.*, 2009, **19**, 7904.
30 O. Osswald, E. Flahaut, H. Ye and Y. Gogotsi, *Chem. Phys. Lett.*, 2005, **402**, 422.